Abdelhamid GHOUL[1], Kamel KARA[1], Selman DJEFFAL[2],
Mohamed BENRABAH[3], Mohamed Laid HADJILI[4]

Artificial neural network for solving the inverse kinematic model of a spatial and planar variable curvature continuum robot

In this paper, neural networks are presented to solve the inverse kinematic models of continuum robots. Firstly, the forward kinematic models are calculated for variable curvature continuum robots. Then, the forward kinematic models are implemented in the neural networks which present the position of the continuum robot's end effector. After that, the inverse kinematic models are solved through neural networks without setting up any constraints. In the same context, to validate the utility of the developed neural networks, various types of trajectories are proposed to be followed by continuum robots. It is found that the developed neural networks are powerful tool to deal with the high complexity of the non-linear equations, in particular when it comes to solving the inverse kinematics model of variable curvature continuum robots. To have a closer look at the efficiency of the developed neural network models during the follow up of the proposed trajectories, 3D simulation examples through Matlab have been carried out with different configurations. It is noteworthy to say that the developed models are a needed tool for real time application since it does not depend on the complexity of the continuum robots' inverse kinematic models.

✉ Abdelhamid GHOUL, email: abdelhamid_ghoul@yahoo.fr

[1]Université of Blida 1, Laboratoire des systèmes électriques et télécommande, Faculty of Technology, Blida, Algeria.

[2]University of Larbi Ben M'hidi, Faculty of Science and Applied Sciences, Oum El Bouaghi, Algeria.

[3]University of Sciences and Technology Houari Boumediene, Laboratoire des systèmes électriques et télécommande, Faculty of Electrical Engineering, Algiers, Algeria.

[4]Haute Ecole Bruxelles, Ecole Supérieure d'Informatique, Brussels, Belgium.

1. Introduction

Labyrinth-like paths, clustered environments where a traditional rigid robot cannot fit the bill due to their rigid links and their inability to adapt to these kinds of paths, thus it would be tempting to find an alternative to these robots. To this end, researchers have developed the so-called continuum bionic robots that are biologically inspired from nature such as tentacle and appendices [1–11], which can easily adapt to any kind of paths thanks to their flexibility and high performance, yet they still present an impediment to researchers, because of their complexity when it comes to modeling, in particular the inverse kinematic model (IKM) of continuum bionic robots. It remains unanswerable despite the fact that many researchers have come up with new methodologies to model them, yet they are not sufficiently reliable and further accuracy is required.

From a modeling point of view, the forward kinematic model (FKM) of continuum robots have been widely proposed for both, continuum bionic robots with constant curvature (CC) [12–15] as well as with variable curvature (VC) [16–18]. For the former ones, the researchers suggest that the robot's each section bends as an arc of circle, while the latter describes the robot's each section as a concatenation of arcs, in other words, each section is a serially connected arcs, each arc owns its bending angle. As far as the IKM is concerned, few works have been developed. In [19], the authors have developed the IKM of one bending section which is based on an active catheter used in surgery. Their model provides unsatisfying results. In [16] the authors have used a velocity based-feed forward motion control to solve the IKM of continuum bionic handling assistant (CBHA) with VC. In [20], the authors have developed specific kinematics of a single section based on an energy modeling technique. Due to the complexity of the analytically developed models to solve the IKM, researchers have switched to using optimization method as well as artificial neural network (ANN) and many other intelligent methods. To emphasize, in [17], the authors have solved the inverse kinematic model of a multi-section continuum robot with VC using particle swarm optimization (PSO) in planar as well as in a spatial case. They formulated the problem of IKM as an objective function, which describes the distance between the robot's end effector and the position on the prescribed trajectory. Similarly, in [21], genetic algorithm (GA) and PSO are applied to solve the IKM of a continuum robot with CC using some constraint conditions. Formulating the IKM of continuum robots as an objective function is handy since the degrees of freedom of the robot are not included in it, thus the meta-heuristic approaches can be extended to be applied on further section of continuum robots. In the other hand, these meta-heuristic approaches show their drawbacks when it comes to real-time applications, for this exact reason, in this paper, an artificial neural network is applied to solve the inverse kinematic model of VC continuum robot for both cases, a spatial single section continuum robot as well as a planar two-section continuum robot with VC. The main advantage of ANN is its simplicity and fast response towards the IKM and to top it up, it can

cover a wide range of trajectories even the ones which were not trained on, namely it can solve the IKM of continuum robots following a random trajectory.

Many works have formulated the problem of using ANN for the CC but for VC, very few works have been proposed. In [22], the inverse kinematic model of a dual-backbone continuum robot is solved using PRBM and ANN. The problem of the IKM in their research is divided into two phases, the first one resides in calculating the forward kinematic model via the PRBM approach then the obtained results are adopted to create an ANN model which aims at solving the IKM. In [23], a learning-based approach is used to deal with the IKM of continuum robots which is based on learning the global solution through supervised learning. The benefit of this method is its ability to come up with solution without knowing any prior information of the system. In [24], Kepler oval is implemented to solve the IKM of inextensible continuum robot. It starts by identifying the workspace of the robot, then it formulates the IKM through a binary equation, which consists of the oval equations, thus its solution is the one of the IKM. The IKM of a multi-section continuum robot is solved through the forward and backward reaching inverse kinematic (FABRIK) algorithm [25]. It is mainly based on reaching out to the targeted point, which paves the way to controlling the robot's end effector orientation, it can be performed through replacing the robot's bending section by a serially connected chords using spherical joints and that occurs during the forward reaching. While in the backward reaching, the algorithm memorizes the arcs, which are obtained from the chords and updated at each iteration.

The main contributions of this paper can be described in; first, creating a database for the FKM of a spatial single section as well as a planar two-section continuum robot with VC. The second part, the implementation of the ANN to solve the IKM is applied on varies types of trajectories. The error between the provided solution by ANN and the desired solution are calculated and depicted through 3D simulations. The rest of the paper is arranged as follows: Section 2 describes the continuum robot design as well as demonstrates the followed methodology to derive the forward kinematic models for variable curvature continuum robot using ANN. Section 3 presents the implementation of the ANN method for solving the inverse kinematic models as well as the identification of its workspace. Section 4 provides with a conclusion and future works.

2. Continuum robot kinematics

The profile of the whole robot is similar to a backbone curve. Each bending section k consists of serially connected units. Every single unit has its own bending and orientation angles, $\theta_{j,k}$ and ϕ_k respectively, which gives birth to the so-called variable curvature continuum robot, see Fig. 1. Each unit is composed of two disks which differ in terms of diameter and each disk has three holes through which the cables pass. Basically, the robot's each section is separately controlled by three cables. Generally, the backbone curve of continuum robots takes two forms, virtual
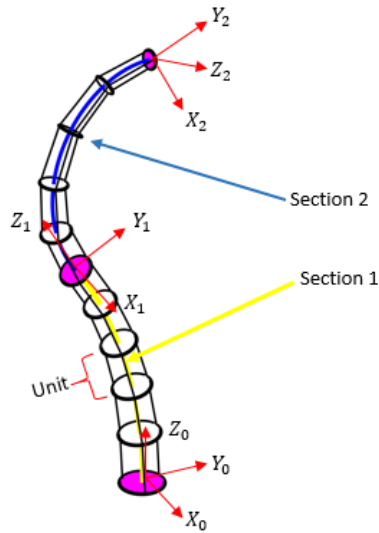
Fig. 1. Two-section continuum robot with its coordinate frames for each section k

as in [16] or a realistic one, which is found in some robots with flexible backbone such as [17, 21] and that considered in this paper. The geometrical parameters of each unit and its kinematics nomenclature are illustrated in Fig. 2 and Table 1.
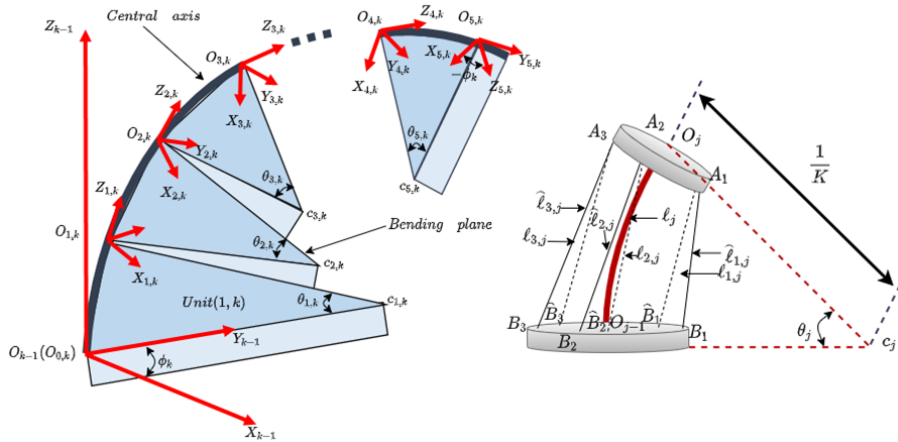

Fig. 2. Description of each unit with its coordinates (left); details of a single unit and its cables (right)

For the constant curvature continuum robot, each unit of the robot has a lower and an upper disk which have the same diameters and connected through the points $A_{i,j,k}$ and $B_{i,j,k}$. For the variable curvature continuum robot, each unit

Table 1. Nomenclature

Symbol	Description
i	the index of cables $i = 1, 2, 3$
j	the index of units $j = 1, 2, ..., 5$
k	the index of sections $k = 1, 2$
$\ell_{i,j}$	the non-conic unit cable length
$\hat{\ell}_{i,j}$	the conical unit cable length
l_j	the length of the central axis of the unit j
$(x, y, z)_{j,k}$	the local coordinate frame
$(X, Y, Z)_k$	the global coordinate frame
$\theta_{j,k}$	the bending angle
ϕ_k	the orientation angle
κ_j	the curvature
r_j	the radial distance between cables and the central axis

has two disks with different diameters and connected through $\widehat{B}_{i,j,k}$ and $A_{i,j,k}$. Interestingly, the differentiation of the disks' diameters paves the way to establishing an equation which relates the units with each other by a ratio as it is explained in detail in [17]. Basically, the development of the used equations in this paper is inspired from [17]. The used assumptions for the modeling of the VC continuum robot along this paper are inspired from the CC [15], which can be summarized as follows:

- The flexible continuum robot is described as an open kinematic chain of n sections.
- Each section is a set of conically equidistant units.
- Each conical shaped unit is modeled as an inextensible circular arc having its individual parameters.
- The cable lengths are homogeneously fragmented along the robot.
- The robot deformations at sections and units are done without torsion (neglected torsion).

2.1. ANN and problem formulation

Neural Networks (NN) have achieved a great success in many areas due to their learning and generalization capabilities as well as their parallelism. They have been successfully used in many applications, such as classification, noise filtering, system modeling and control, etc. One of the fields where NN has received an increasing interest is that of solving the robots' inverse kinematics models.

Due to the complexity of variable curvature continuum robots models, very few works which aim at solving their IKMs have been carried out. To this end, the Multi-Layer Perceptron (MLP) neural networks are used and developed to find the IKMs of a single as well as a two-section continuum robot with variable curvature. The hidden layers contains neurons with sigmoid activation function and a linear

activation function in output layers. For the sake of avoiding the complexity of the neural networks a minimum number of neurons and hidden layers that gives the good learning are chosen.

The forward kinematic model is calculated for the sake of obtaining the P_{x_i}, P_{y_i}, and P_{z_i} coordinates of the robot's end tip which themselves are used to train the proposed MLP. The problem of IKM in this paper can be expressed by equation (1), as follows:

$$F = \frac{1}{N} \sum_{i=1}^{N} \left((P_{x_i} - X_{c_i})^2 + (P_{y_i} - Y_{c_i})^2 + (P_{z_i} - Z_{c_i})^2 \right), \tag{1}$$

where N represent the number of data. X_{c_i}, Y_{c_i}, and Z_{c_i} represent the spatial coordinates of a located position on the prescribed trajectory. P_{x_i}, P_{y_i}, and P_{z_i} represent the position of the robot's end tip for each specific position of the prescribed trajectory, which are obtained from the FKM. Explicitly, they present the three first components of the forth column of the following matrix:

$$\mathbf{T}_n^0 = \prod_n^0 \mathbf{T}_{j,k}^{j-1,k}, \tag{2}$$

in which

$$\mathbf{T}_{j,k}^{j-1,k} = \left(\begin{array}{c|c} \mathbf{R}_{j,k}^{j-1,k} & \mathbf{P}_{j,k}^{j-1,k} \\ \hline \mathbf{0}_{1\times3} & 1 \end{array} \right), \tag{3}$$

where $\mathbf{R}_{j,k}^{j-1,k}$ and $\mathbf{P}_{j,k}^{j-1,k}$ are the rotational matrix and the vector position, respectively. They can be expressed as a function of arc parameters as follows:

$$\mathbf{R}_{j,k}^{j-1,k} = \mathbf{rot}(Z_{j-1,k}, \phi_k) \cdot \mathbf{rot}(Y_{j-1,k}, \theta_{j,k}) \cdot \mathbf{rot}(Z_{j-1,k}, -\phi_k), \tag{4}$$

$$\mathbf{P}_{j,k}^{j-1,k} = \begin{cases} \dfrac{l_{j,k}}{\theta_{j,k}}(1 - \cos(\theta_{j,k}))\cos(\phi_k), \\[2mm] \dfrac{l_{j,k}}{\theta_{j,k}}(1 - \cos(\theta_{j,k}))\sin(\phi_k), \\[2mm] \dfrac{l_{j,k}}{\theta_{j,k}}\sin(\theta_{j,k}), \end{cases} \tag{5}$$

and the bending angle $\theta_{j,k}$ is given as a function of the first bending angle θ_1 as follows [17]:

$$\theta_{j,k} = \frac{r_{1,k}}{r_{j,k}}\theta_{1,k}. \tag{6}$$

Since the treated continuum robot in this work is actuated by cables, it is crucially important to calculate its cables length during the follow up of a specific

trajectory for the sake of evaluating the behavior of cables when the robot bends. The equation which can express the cables length for a variable curvature continuum robot is as follows [16]:

$$\ell_{i,j,k} = \sqrt{\widehat{\ell}_{i,j,k} - \left(r_{j-1,k} - r_{j,k}\right)^2} \, . \tag{7}$$

The diameters of the disks can be calculated using equation [17]:

$$r_{j,k} = r_{\max,k} - \frac{j}{k}\left(r_{\max,k} - r_{\min,k}\right) \, . \tag{8}$$

3. Outline and simulation

In this paper, two simulations examples are considered, for the first simulation; a single spatial section continuum robot with variable curvature is ordered to follow up two types of trajectories, namely, arc-shaped trajectory as well as a circular trajectory.

For the second simulation, a planar two-section continuum robot with variable curvature is ordered to follow up two types of trajectories, linear trajectory and an arc-shaped trajectory. The characteristics of the considered robot are demonstrated in Table 2.

Table 2. The parameters of the considered flexible continuum robot

Parameter	Section 1	Section 2	Description
m_k	5 units	5 units	Number of units
l_k	300 mm	300 mm	Total length of the section
$r_{\min,k}$	17.5 mm	10 mm	Radial distance of the cable
$r_{\max,k}$	25 mm	17.5 mm	Radial distance of the cable

Furthermore, it has been shown in several works that a neural network with one or two hidden layers is sufficient to approximate any nonlinear function [26–29]. For the sake of simplicity, one hidden layer for a single-section continuum robot and two hidden layers for two section continuum robot are used as well as a minimum number of neurons that gives good learning and that reflects back on the robot's accuracy during trajectory tracking.

The whole process has been performed in Matlab 2018a software with the following characteristics: an Intel Core i7, 3.60 GHz, 4 GB RAM.

3.1. IKM of spatial single section continuum robot

Variable curvature continuum robots suffer from the complexity of their kinematic models, especially when including rotation angles, which makes the neural network unable to learn in the presence of rotation angles. Therefore, the rotation

angles are first calculated mathematically in order to know the direction of the robot in its workspace. Then, to give the neural network more information for good learning about the problem, the rotation angles are given along with the Cartesian coordinates as inputs to extract the bending angles with more accuracy.

The FKM of a spatial single section is first calculated using equation (2), and the orientation angle is then calculated analytically using FKM by dividing the position P_y by the position P_x. Finally, the static MLP (Fig. 3) with the following configuration is used to calculate the bending angles:

- The input layer contains four inputs (x, y, z, ϕ).
- One hidden layer with 20 neurons.
- One linear output neuron that gives the approximated θ.
- Learning rate: $\alpha = 0.01$.
- Type of optimizer: Levenberg-Marquardt backpropagation.
- Loss function: MSE.
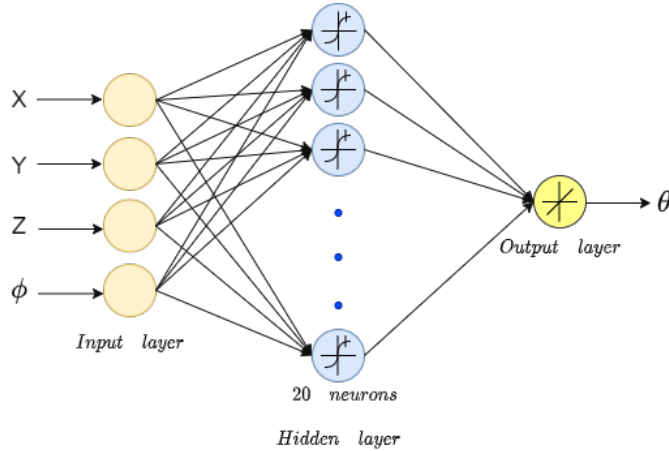
Fig. 3. Neural structure spatial single section continuum robot

A dataset with 10000 random samples (values) is generated using the FKM to train the developed model as follows:

1. Random values for the bending and rotation angles that covers all-inclusive possible positions in the robot's workspace are created using the following two equations:

$$\begin{cases} \theta_i = \text{rand}(\theta_{\max} - \theta_{\min}) + \theta_{\min}, \\ \phi_i = \text{rand}(\phi_{\max} - \phi_{\min}) + \phi_{\min}, \end{cases} \tag{9}$$

where: $\theta_{\max} = \dfrac{\pi}{8}$; $\theta_{\min} = -\dfrac{\pi}{8}$; $\phi_{\max} = \pi$; $\phi_{\min} = -\pi$.

2. The bending and rotation angles created using the FKM are applied to calculate the corresponding Cartesian coordinates (x_i, y_i, z_i).

3. Finally, Cartesian coordinates and rotation angles are saved as inputs, and bending angles as outputs.

The training performance result error value to the bending angle is given by Fig. 4.
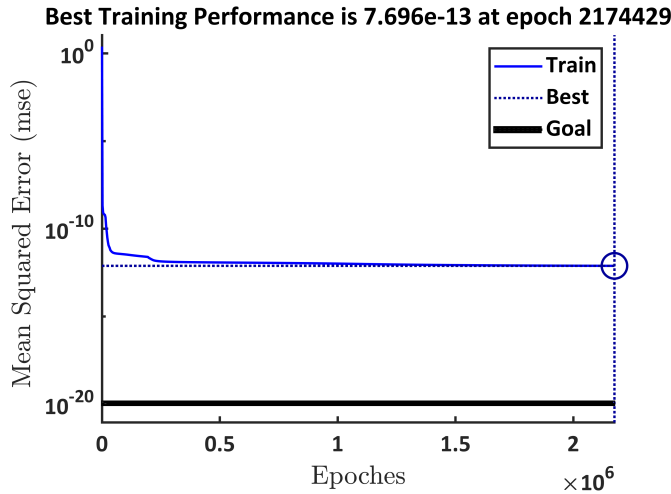

Fig. 4. Training performance error (MSE) results of the neural model for the bending angle θ

Following the same previous steps, a second database with 10000 random values that cover all-inclusive possible positions in the robot's workspace is generated to evaluate the effectiveness of the obtained IKM. Fig. 5 gives the error test results of the developed neural model for the bending angle θ.
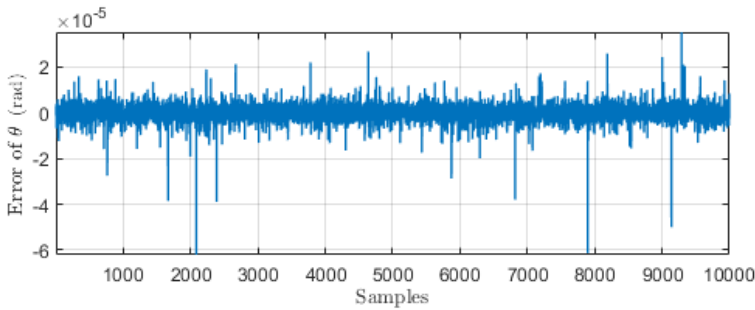
Fig. 5. Error test results of the neural model for the bending angle θ

After tested the effectiveness of the obtained model (IKM), the considered robot is tested on practically realistic-like trajectories (circular and arc-shaped trajectories) in order to assess the robot's behavior via 3D simulations.

As it is shown in Fig. 6, the considered single section continuum robot with VC can accurately follow the arc-shaped trajectory within its 3D workspace (yellow curved arcs).
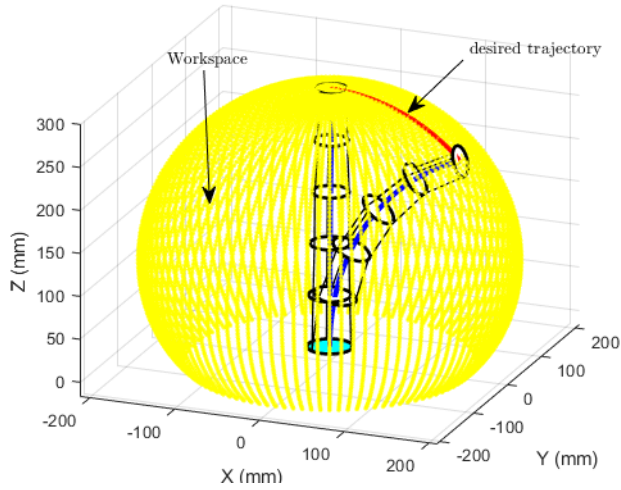
Fig. 6. Two configurations of a single section continuum robot following
an arc shaped trajectory within its 3D workspace

To show the accuracy of the generated trajectory, Euclidean errors are calcu-
lated. As it is shown in Fig. 7, the maximum error between the generated and the
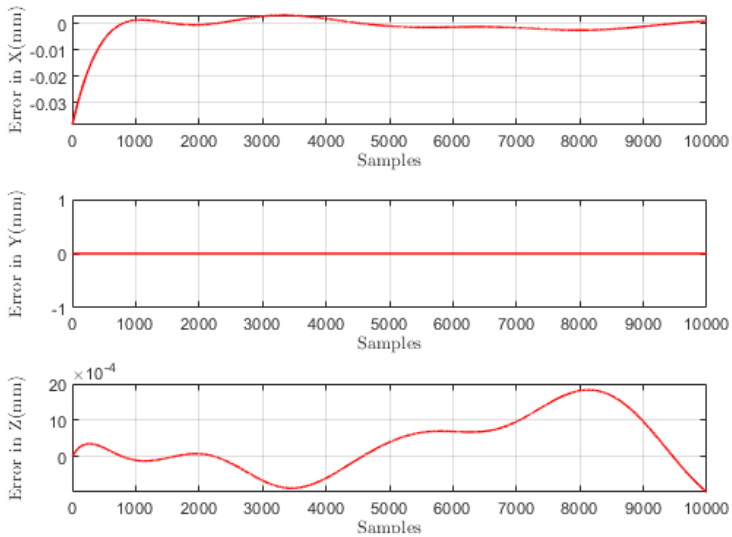desired trajectory is of the order of 0.002 mm.

Fig. 7. Error between the reference trajectory (arc-shaped) and the trajectory (arc-shaped)
given by the NN

Similarly to the first simulation example, the continuum robot tracks a circular
trajectory within its workspace (Fig. 8). Fig. 9 shows the Euclidean error of the
trained NN.
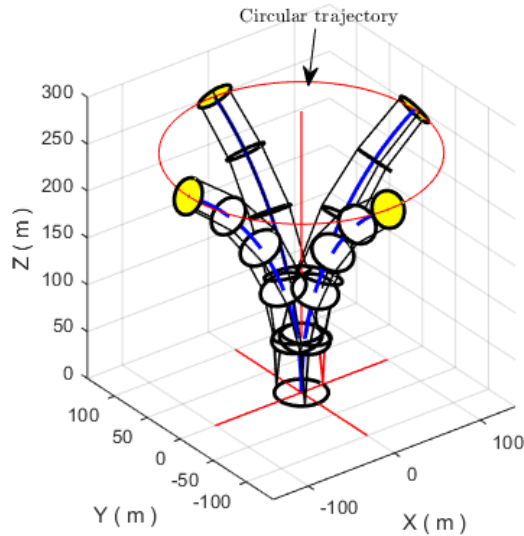
Fig. 8. Representation of the continuum robot's first section
tracking the desired circular trajectory
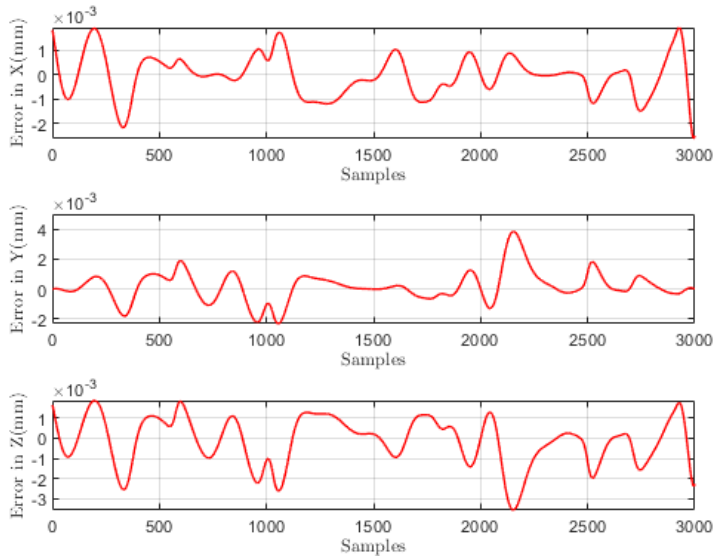
Fig. 9. Error between the reference circular trajectory and the circular trajectory given by the NN

3.2. IKM of planar two-section continuum robot

In the second simulation, two databases with 10000 values have been created from the FKM of a two-section VC continuum robot using random values of the bending angles within the robot's workspace. After that, to calculate the IKM of the

considered robot, an ANN with two hidden layers is built up (Fig. 10). Using the generated data, the error between the generated bending angles and angles obtained from the trained NN is shown in Fig. 11.
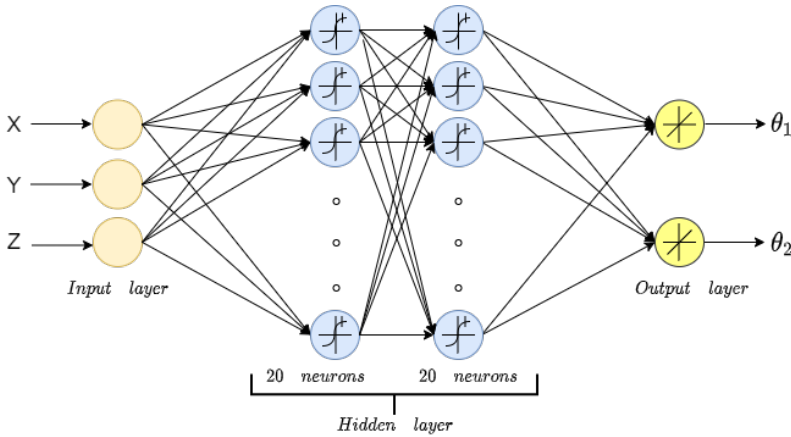
Fig. 10. The architecture of the neural model for a planer two-section continuum robot

The value of the mean square error (MSE) of the achieved model are given in Fig. 11.
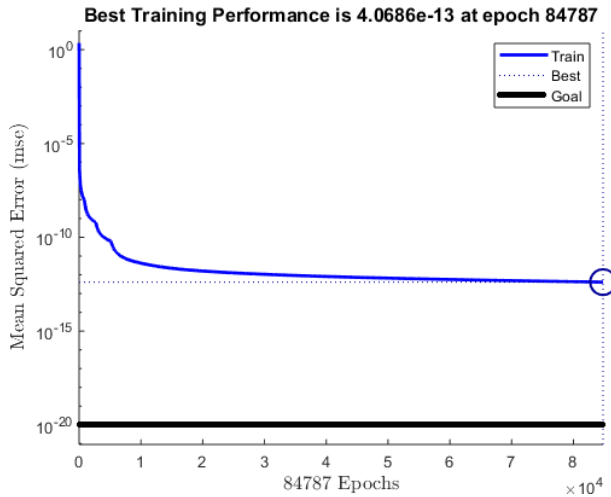
Fig. 11. Training performance results (MSE) of the neural model
for the two-section continuum robot

Finally, the IKM accuracy is evaluated by applying the second created database, and the error in its bending angles is shown in Fig. 12.
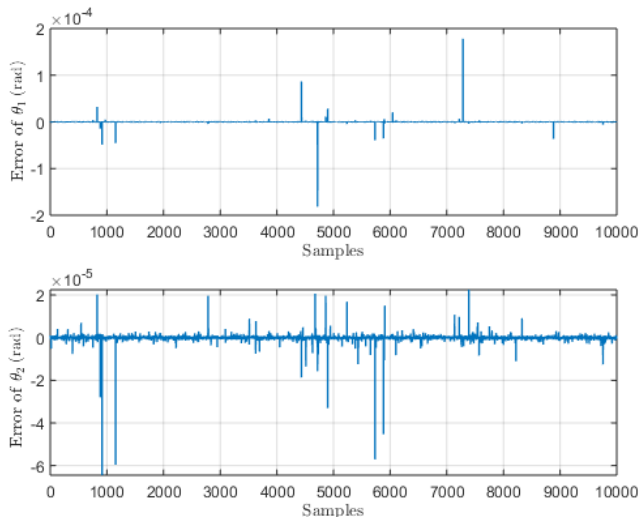
Fig. 12. Test results of the obtained model for the two-section continuum robot

Fig. 13 shows that the considered two-section continuum robot with variable curvature can accurately follow the linear trajectory expressed by equation (10):

$$\begin{cases} X = 10t + 200 \,, \\ Y = 0 \,, \\ Z = 370 - 4t \,, \end{cases} \tag{10}$$

with $t = 0{:}0.1{:}15$.

It is noteworthy to say that each position on the linear trajectory can be reached by the robot's end-effector through at least three configurations (redundancy), as it
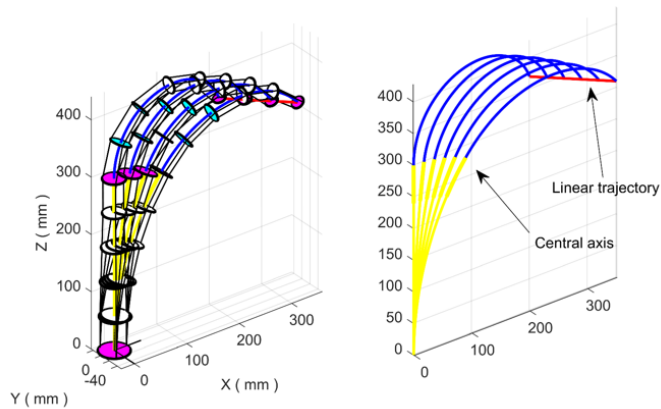
Fig. 13. Different configurations for the robot following the linear trajectory
with respect the minimum curvature norm (left); central axis of the robot
following the linear trajectory (right)

is shown in Fig. 14. Therefore, only one existing configuration (solution) is taken which allows the robot to track the linear trajectory and that can be achieved by adding constraints to the objective function during the learning phase according to many norms such as velocity sensitivity and minimum curvature, etc., [30, 31]. In this work, the minimum curvature norm is chosen with the aim of keeping the robot from more undesirable curvatures. To emphasize, through the added constraints only one solution can be considered which allows the robot to reach the specific position through one configuration as shown in Fig. 13.
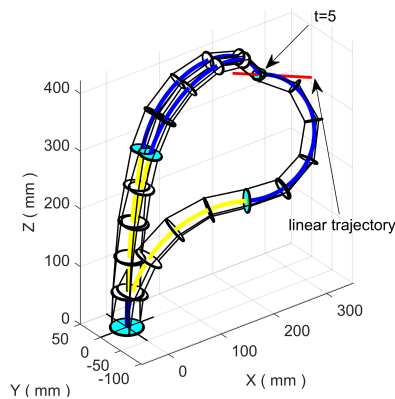
Fig. 14. Possible solutions for each desired point on the linear trajectory (redundancy)

The Euclidean error between the generated and the desired linear trajectory is shown in Fig. 15.
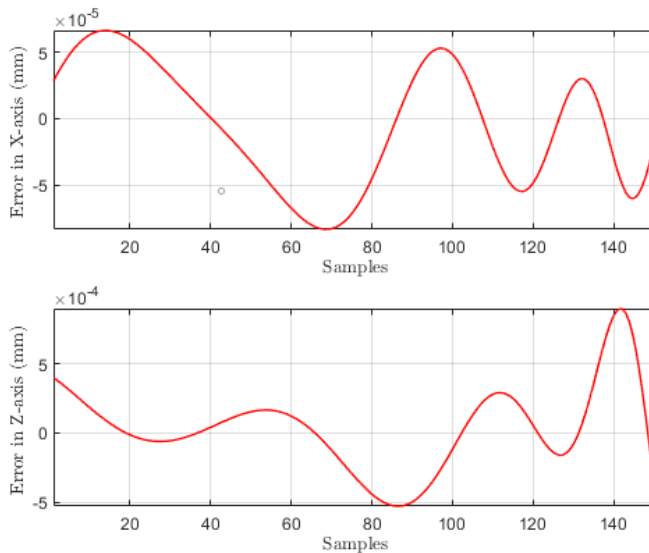

Fig. 15. Euclidean errors between the desired and the obtained trajectory (linear trajectory)

In the last simulation, an arc-shaped trajectory is followed up by a two-section continuum robot, as shown in Fig. 16. This kind of trajectory is deliberately used since it allows the robot to considerably bend and in order to assess the NN when dealing with large bending angles (Fig. 17). Furthermore, the cables length are calculated based on the bending angles (Fig. 18) which are provided by the obtained NN, as it is shown in Fig. 19.
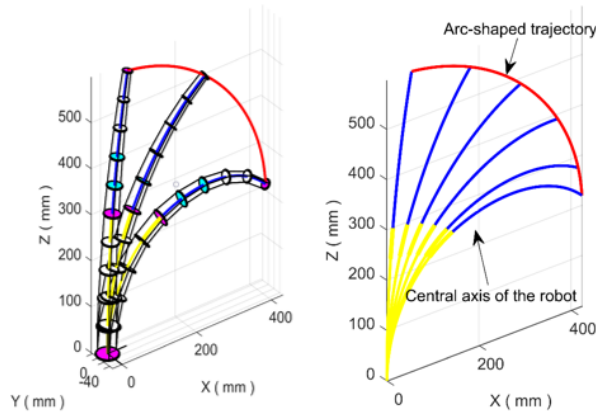

Fig. 16. Different configuration for the robot following the arc-shaped trajectory (left);
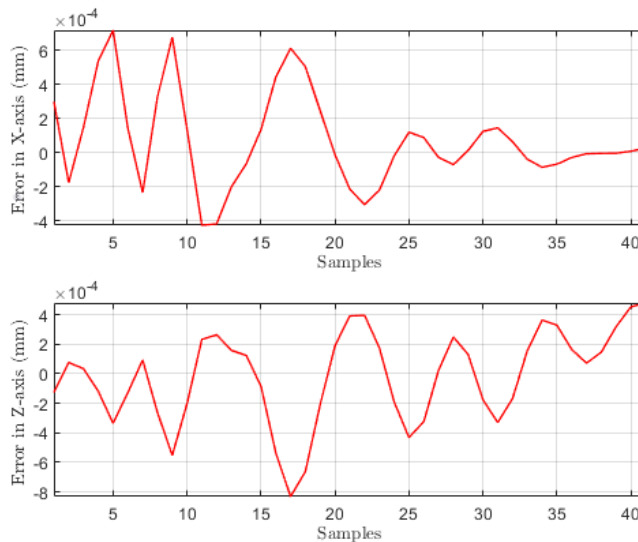central axis of the robot following the arc-shaped trajectory (right)

Fig. 17. Euclidean errors between the desired and the obtained trajectory
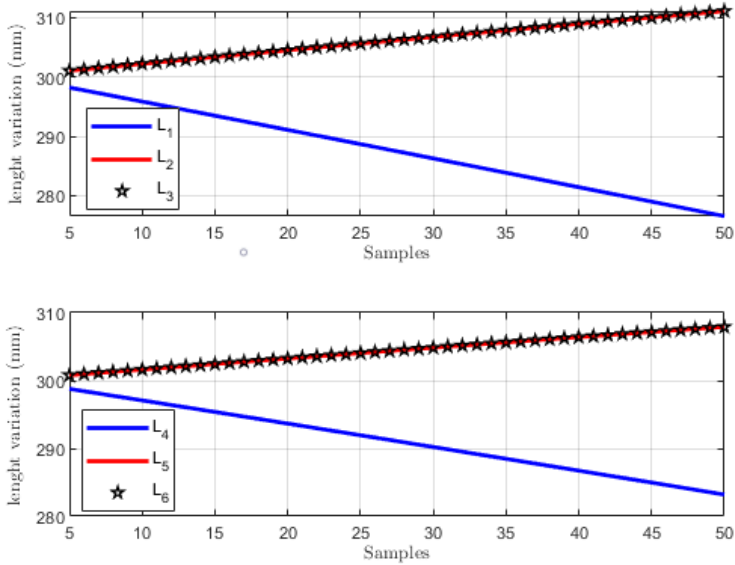(arc-shaped) for the two-section continuum robot

Fig. 18. Lengths variation of the two-section continuum robot while tracking
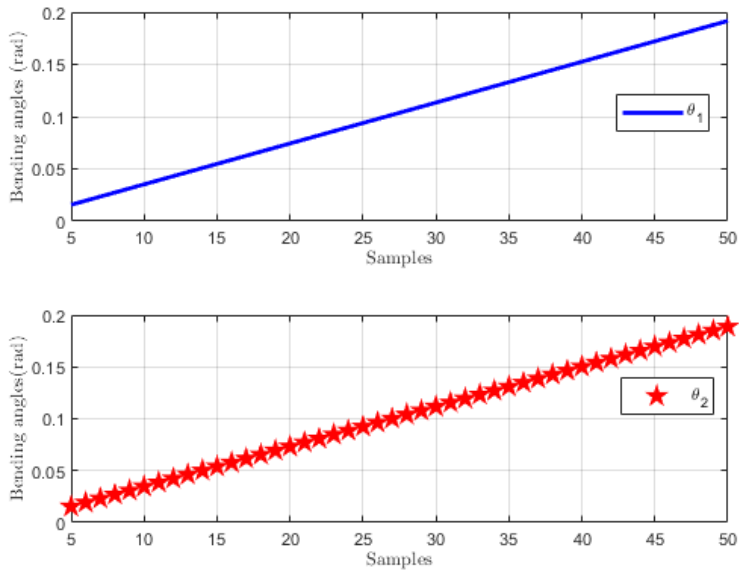the arc-shaped trajectory

Fig. 19. Needed bending angles for the two-section continuum robot following
the arc-shaped trajectory

Although the tackled trajectory which is shown in Fig. 16 is relatively difficult
compared to the previously proposed trajectories, the NN IKM gives satisfactory
tracking accuracy (Fig. 17).

4. Conclusion

In this paper, artificial neural networks are used to solve the inverse kinematic model of variable curvature continuum robots. The established inverse kinematic-based neural network does not depend on the highly non-linearity of continuum robot's equations, namely, the forward kinematic model is used to build up a database which is then adopted to train the neural network model. The obtained database for training the neural model covers all-inclusive and reachable positions within the robot's workspace. To emphasize, the database contains the Cartesian coordinate of the robot's end effector as inputs and the bending angles as outputs therefore, for a given trajectory the robot's end effector can predict the needed bending angle since it has been trained throughout its whole workspace allowing the robot to reach to any position on the prescribed trajectory. Basically, through the performed simulations dedicated to trajectory tracking, neural network can be considered as an alternative to solving the inverse kinematic model with a remarkable accuracy without any prior knowledge of the equations related to the inverse kinematic model. Furthermore, it is crucially important to say that the ANN is an appropriate tool to deal with real time application on the contrary to other meta-heuristic approaches, namely their accuracy is good but they do not respond to the needs which are required by industry and that can be shown in the real time application. The potential work for the developed ANN can reside in solving the inverse kinematic model of variable curvature with the presence of torsion and variable length since the ANN has nothing to do with the complexity of the IKM model.

Acknowledgements

References

[1] D. Trivedi, C.D. Rahn, W.M. Kier, and I.D. Walker. Soft robotics: Biological inspiration, state of the art, and future research. *Applied Bionics and Biomechanics*, 5(3):99–117, 2008. doi: 10.1080/11762320802557865.

[2] G. Robinson and J.B.C. Davies. Continuum robots – a state of the art. In *Proceedings 1999 IEEE International Conference on Robotics and Automation*, volume 4, pages 2849–2854, 1999. doi: 10.1109/ROBOT.1999.774029.

[3] I.D. Walker. Continuous backbone "continuum" robot manipulators. *International Scholarly Research Notices*, 2013:726506, 2013. doi: 10.5402/2013/726506.

[4] H.-S. Yoon and B.-J. Yi. Development of a 4-DOF continuum robot using a spring backbone. *The Journal of Korea Robotics Society*, 3(4):323–330, 2008.

[5] M. Li, R. Kang, S. Geng, and E. Guglielmino. Design and control of a tendon-driven continuum robot. *Transactions of the Institute of Measurement and Control*, 40(11):3263–3272, 2018. doi: 10.1177/0142331216685607.

[6] G. Gao, H. Wang, J. Fan, Q. Xia, L. Li, and H. Ren. Study on stretch-retractable single-section continuum manipulator. *Advanced Robotics*, 33(1):1–12, 2019. doi: 10.1080/01691864.2018.1554507.

[7] C. Laschi, B. Mazzolai, V. Mattoli, M. Cianchetti, and P. Dario. Design of a biomimetic robotic octopus arm. *Bioinspiration & Biomimetics*, 4(1):15006, 2009. doi: 10.1088/1748-3182/4/1/015006.

[8] F. Renda, M. Cianchetti, M. Giorelli, A. Arienti, and C. Laschi. A 3D steady-state model of a tendon-driven continuum soft manipulator inspired by the octopus arm. *Bioinspiration & Biomimetics*, 7(2):25006, 2012. doi: 10.1088/1748-3182/7/2/025006.

[9] F. Renda, M. Giorelli, M. Calisti, M. Cianchetti, and C. Laschi. Dynamic model of a multi-bending soft robot arm driven by cables. *IEEE Transactions on Robotics*, 30(5):1109–1122, 2014. doi: 10.1109/TRO.2014.2325992.

[10] Y. Peng, Y. Liu, Y. Yang, N. Liu, Y. Sun, Y. Liu, H. Pu, S. Xie, and J. Luo. Development of continuum manipulator actuated by thin McKibben pneumatic artificial muscle. *Mechatronics*, 60:56–65, 2019. doi: 10.1016/j.mechatronics.2019.05.001.

[11] G. Gao, H. Ren, Q. Xia, H. Wang, and L. Li. Stretched backboneless continuum manipulator driven by cannula tendons. *Industrial Robot*, 45(2):237–243, 2018. doi: 10.1108/IR-06-2017-0124.

[12] R.J. Webster III and B.A. Jones. Design and kinematic modeling of constant curvature continuum robots: A review. *The International Journal of Robotics Research*, 29(13):1661–1683, 2010. doi: 10.1177/0278364910368147.

[13] S. Mosqueda, Y. Moncada, C. Murrugarra, and H. León-Rodriguez. Constant curvature kinematic model analysis and experimental validation for tendon driven continuum manipulators. In *Proceedings of the 15th International Conference on Informatics in Control, Automation and Robotics ICINCO (2)*, volume 2, pages 211–218, 2018. doi: 10.5220/0006913502110218.

[14] A. Ghoul, K. Kara, M. Benrabah, and M.L. Hadjili. Optimized nonlinear sliding mode control of a continuum robot manipulator. *Journal of Control, Automation and Electrical Systems*, pages 1–9, 2022. doi: 10.1007/s40313-022-00914-1.

[15] C. Escande. *Towards Modeling of a Class of Bionic Manipulator Robots*. PhD Thesis, Lille, France, 2013.

[16] T. Mahl, A. Hildebrandt, and O. Sawodny. A variable curvature continuum kinematics for kinematic control of the bionic handling assistant. *IEEE Transactions on Robotics*, 30(4):935–949, 2014. doi: 10.1109/TRO.2014.2314777.

[17] S. Djeffal, A. Amouri, and C. Mahfoudi. Kinematics modeling and simulation analysis of variable curvature kinematics continuum robots. *UPB Scientific Bulletin, Series D: Mechanical Engineering*, 83:28–42, 2021.

[18] S. Djeffal, C. Mahfoudi, and A. Amouri. Comparison of three meta-heuristic algorithms for solving inverse kinematics problems of variable curvature continuum robots. In *2021 European Conference on Mobile Robots (ECMR)*, pages 1–6, 2021. doi: 10.1109/ECMR50962.2021.9568789.

[19] O. Lakhal, A. Melingui, A. Shahabi, C. Escande, and R. Merzouki. Inverse kinematic modeling of a class of continuum bionic handling arm. In *2014 IEEE/ASME International Conference on Advanced Intelligent Mechatronics*, pages 1337–1342, 2014. doi: 10.1109/AIM.2014.6878268.

[20] D. Trivedi, A. Lotfi, and C.D. Rahn. Geometrically exact dynamic models for soft robotic manipulators. In *2007 IEEE/RSJ International Conference on Intelligent Robots and Systems*, pages 1497–1502, 2007. doi: 10.1109/IROS.2007.4399446.

[21] A. Amouri, C. Mahfoudi, A. Zaatri, O. Lakhal, and R. Merzouki. A metaheuristic approach to solve inverse kinematics of continuum manipulators. *Proceedings of the Institution of Mechanical Engineers, Part I: Journal of Systems and Control Engineering*, 231(5):380–394, 2017. doi: 10.1177/0959651817700779.

[22] E. Shahabi and C.-H. Kuo. Solving inverse kinematics of a planar dual-backbone continuum robot using neural network. In B. Corves, P. Wenger, and M. Hüsing, editors, *EuCoMeS 2018*, pages 355–361. Springer, Cham, 2019. doi: 10.1007/978-3-319-98020-1_42.

[23] T.G. Thuruthel, E. Falotico, M. Cianchetti, and C. Laschi. Learning global inverse kinematics solutions for a continuum robot. In V. Parenti-Castelli and W. Schiehlen, editors, *ROMANSY 21 - Robot Design, Dynamics and Control*, pages 47–54. Springer, Cham, 2016. doi: 10.1007/978-3-319-33714-2_6.

[24] L. Jiajia, D. Fuxin, L. Yibin, L. Yanqiang, Z. Tao, and Z. Gang. A novel inverse kinematics algorithm using the Kepler oval for continuum robots. *Applied Mathematical Modelling*, 93:206–225, 2021. doi: 10.1016/j.apm.2020.12.014.

[25] D.Y. Kolpashchikov, N.V. Laptev, V.V. Danilov, I.P. Skirnevskiy, R.A. Manakov, and O.M. Gerget. FABRIK-based inverse kinematics for multi-section continuum robots. In *2018 18th International Conference on Mechatronics-Mechatronika (ME)*, pages 1–8. IEEE, 2018.

[26] R. Köker, C. Öz, T. Çakar, and H. Ekiz. A study of neural network based inverse kinematics solution for a three-joint robot. *Robotics and Autonomous Systems*, 49(3-4):227–234, 2004. doi: 10.1016/j.robot.2004.09.010.

[27] R.Y. Putra, S. Kautsar, R.Y. Adhitya, M. Syai'in, N. Rinanto, I. Munadhif, S.T. Sarena, J. En-drasmono, and A. Soeprijanto. Neural network implementation for invers kinematic model of arm drawing robot. In *2016 International Symposium on Electronics and Smart Devices (ISESD)*, pages 153–157, 2016. doi: 10.1109/ISESD.2016.7886710.

[28] N. Bigdeli, K. Afsar, B.I. Lame, and A. Zohrabi. Modeling of a five link biped robot dynamics using neural networks. *Journal of Applied Sciences*, 8(20):3612–3620, 2008.

[29] Z. Bingul, H.M. Ertunc, and C. Oysu. Comparison of inverse kinematics solutions using neural network for 6r robot manipulator with offset. In *2005 ICSC Congress on Computational Intelligence Methods and Applications*, page 5, 2005. doi: 10.1109/CIMA.2005.1662342.

[30] X. Zhang, Y. Liu, D.T. Branson, C. Yang, J. S Dai, and R. Kang. Variable-gain control for continuum robots based on velocity sensitivity. *Mechanism and Machine Theory*, 168:104618, 2022. doi: 10.1016/j.mechmachtheory.2021.104618.

[31] A. Liegeois. Automatic supervisory control of the configuration and behavior of multibody mechanisms. *IEEE Transactions on Systems, Man, and Cybernetics*, 7(12):868–871, 1977.